

# Fractional revivals through Rényi uncertainty relations

E. Romera<sup>1,2</sup> and F. de los Santos<sup>1,3</sup>

<sup>1</sup> *Instituto Carlos I de Física Teórica y Computacional,  
Universidad de Granada, Fuentenueva s/n, 18071 Granada, Spain*

<sup>2</sup> *Departamento de Física Atómica, Molecular y Nuclear,  
Universidad de Granada, Fuentenueva s/n, 18071 Granada, Spain*

<sup>3</sup> *Departamento de Electromagnetismo y Física de la Materia,  
Universidad de Granada, Fuentenueva s/n, 18071 Granada, Spain*

(Dated: September 22, 2014)

We show that the Rényi uncertainty relations give a good description of the dynamical behavior of wave packets and constitute a sound approach to revival phenomena by analyzing three model systems: the simple harmonic oscillator, the infinite square well, and the quantum bouncer. We prove the usefulness of entropic uncertainty relations as a tool for identifying fractional revivals by providing a comparison in different contexts with the usual Heisenberg uncertainty relation and with the common approach in terms of the autocorrelation function.

PACS numbers: 03.65.Ge;03.65.Sq

## I. INTRODUCTION

The temporal evolution of wave packets displays a wide variety of non-classical effects and, in this regard, revivals and fractional revivals have raised great interest during the last years [1]. Revivals occur when a wave packet solution of the Schrödinger equation returns to a state that closely reproduces its initial wave form, at multiples of a revival time  $T_{\text{rev}}$ . Fractional revivals appear as the temporal self-splitting of the initial wave packet into a collection of a number of scaled copies. Assuming that the initial state is a superposition of eigenstates  $u_n(x)$  sharply peaked around some  $n_0$ , revival times can then be obtained from the Taylor series of the energy spectrum  $E_n$  around  $E_{n_0}$

$$E_n \approx E_{n_0} + E'_{n_0}(n - n_0) + \frac{E''_{n_0}}{2}(n - n_0)^2 + \dots \quad (1)$$

as  $T_{\text{rev}} = 2\hbar/|E''_{n_0}|$ . Fractional revival times are given by rational fractions of the revival time [2–4]. These phenomena have been observed in many experimental situations and studied theoretically in a variety of quantum systems such as Rydberg wave packets in atoms and molecules, Bose-Einstein condensates, etc [1–6]. Interestingly, the phenomenon of revivals is at the basis of a method for isotope separation [7] as well as for number factorization [8].

Revivals and fractional revivals are usually quantified using the autocorrelation function

$$A(t) \equiv \int_{-\infty}^{\infty} \psi^*(x, t) \psi(x, 0) dx = \int_{-\infty}^{\infty} \phi^*(p, t) \phi(p, 0) dp, \quad (2)$$

which is the overlap between the initial and the time-evolving wave packet in either the position or momentum representation. Given an initial state,  $A(t)$  decreases in time and the occurrence of revivals reflects in the return of  $A(t)$  to its initial value of unity, or in the appearance of relative maxima in the case of fractional revivals.

Revival phenomena have been studied as well by tracking the time evolution of the expectation values of some quantities [4, 9, 10], and an approach based on a finite difference eigenvalue method has been recently put forward from which the various orders of revivals can be directly calculated rather than searching for them [11].

Recently, the sum of Shannon information entropies in position and momentum conjugate spaces has been shown to provide a useful tool for describing fractional revivals, complementary to the usual approach in terms of the autocorrelation function [12]. The underlying idea is that the position-space Shannon entropy measures the uncertainty in the localization of the particle in space [26], so the lower is this entropy the more concentrated is the probability density  $|\psi(x, t)|^2$ , the smaller is the uncertainty, and the higher is the accuracy in predicting the localization of the particle. Equivalently, the momentum-space entropy measures the uncertainty in predicting the momentum of the particle. Thus, the sum of Shannon entropies gives an account of the spreading (high entropy values) and the regenerating (low entropy values) of initially well localized wave packets during the time evolution, and the temporary formation of fractional revivals of the wave function is given by the relative minima of the sum of Shannon information entropies in both conjugate spaces due to the fact that the uncertainty relation is saturated only for Gaussian wave packets [12].

In this article, we expand on the entropic uncertainty approach by describing fractional revivals by means of the sum of the Rényi entropies in position and momentum conjugate spaces, and make a comparison with an analysis based on the time evolution of the standard uncertainty relation in terms of the variance of the probability density in both position and momentum spaces. In the next section we review some basic properties of the Rényi entropy and apply it to three specific model systems: the harmonic oscillator, which can be worked out analytically; the infinite square well, which exhibits perfect revival behavior, and the quantum bouncer, which

has been recently realized using neutrons [13] and atomic clouds [14]

## II. FRACTIONAL REVIVALS AND THE RÉNYI UNCERTAINTY RELATION

The Rényi entropy is a generalization of the Shannon entropy and has been widely employed in the study of quantum systems. Among others applications, it was used in the analysis of quantum entanglement [15], quantum communication protocols [16], localization properties of Rydberg states and spin systems [17], and quantum measurement and decoherence [18]. It is defined in terms of a general probability density  $f(x)$  as (see [19] and references therein)

$$R_f^{(\alpha)} \equiv \frac{1}{1-\alpha} \ln \int_{-\infty}^{\infty} [f(x)]^{\alpha} dx \quad \text{for } 0 < \alpha < \infty \quad \alpha \neq 1. \quad (3)$$

In terms of the probability density in position and momentum spaces,  $\rho(x) = |\phi(x)|^2$  and  $\gamma(p) = |\phi(p)|^2$ , respectively, the Rényi uncertainty relation is given by [19]

$$R_{\rho}^{(\alpha)} + R_{\gamma}^{(\beta)} \geq -\frac{1}{2(1-\alpha)} \ln \frac{\alpha}{\pi} - \frac{1}{2(1-\beta)} \ln \frac{\beta}{\pi} \quad (4)$$

where  $1/\alpha + 1/\beta = 2$ . From the continuous or integral Rényi entropy, as defined in equation (3), it is straightforward to obtain the following limiting behaviors

$$\begin{aligned} R_f^{(\alpha)} &\xrightarrow{\alpha \rightarrow 1} S_f \equiv - \int f(x) \ln f(x) dx, \\ R_f^{(\alpha)} &\xrightarrow{\alpha \rightarrow \infty} - \ln[\max_x f(x)]. \end{aligned} \quad (5)$$

Consequently, in the limits  $\alpha \rightarrow 1$  and  $\beta \rightarrow 1$  the Rényi uncertainty relation (4) reduces to Shannon's [20],

$$S_{\rho} + S_{\gamma} \geq 1 + \ln(\pi) \quad (6)$$

which can thus be considered a particular case of the former. Clearly, all of the above discussion on the benefits of using the Shannon entropy to study revival phenomena carries over to the Rényi entropy as well. It is noteworthy, however, that at the core of the success of the entropic approach is the existence of the uncertainty relations (4) and (6). For this same reason, it is expected that insights on fractional revivals can also be gleaned from the standard variance-based Heisenberg uncertainty relation, which in the case of the usual position and momentum variables leads to the celebrated inequality [21]

$$\Delta x \Delta p \geq \frac{\hbar}{2}, \quad (7)$$

with  $(\Delta x)^2 = \langle x^2 \rangle - \langle x \rangle^2$  and  $(\Delta p)^2 = \langle p^2 \rangle - \langle p \rangle^2$ . Note that inequalities (4) and (6) are saturated by Gaussian probability distributions.

Next, we make use of the relations (4) and (7) to study revival and fractional revivals in three illustrative cases.

### A. Simple harmonic oscillator

The harmonic oscillator provides the most straightforward example of a system showing bound states for which the periodic motion of wave packet solutions (especially Gaussian) is easily derivable. In the present case  $V(x) = \frac{1}{2}m\omega^2 x^2$  and all wave packet solutions, Gaussian or not, satisfy  $\psi(x, t + mT_{cl}) = (-1)^m \psi(x, t)$ , where  $T_{cl} = 2\pi/\omega$  is the classical period. The associated time dependent expectation values  $\langle x \rangle_t$  and  $\langle p \rangle_t$  behave exactly as for a classical particle [4, 23],

$$\begin{aligned} \langle x \rangle_t &= \langle x \rangle_0 \cos(\omega t) + \frac{\langle p \rangle_0}{m\omega} \sin(\omega t), \\ \langle p \rangle_t &= -m\omega^2 \langle x \rangle_0 \sin(\omega t) + \langle p \rangle_0 \cos(\omega t). \end{aligned} \quad (8)$$

The behavior of the uncertainties can also be worked out explicitly. For our purposes, it suffices to focus on initial Gaussian wave functions, also known as squeezed states,

$$\psi(x, 0) = \frac{1}{\sqrt{\sigma\sqrt{\pi}}} e^{ip_0 x/\hbar} e^{-(x-x_0)^2/2\sigma^2}. \quad (9)$$

The time-evolved wave function is then given in closed form for arbitrary times as [4]

$$\psi(x, t) = \frac{1}{\sqrt{|L(t)|}\sqrt{\pi}} e^{\frac{S(x,t)}{2\sigma L(t)}} \quad (10)$$

with

$$L(t) = \sigma \cos(\omega t) + \frac{i\hbar}{m\omega\sigma} \sin(\omega t) \quad (11)$$

and

$$\begin{aligned} S(x, t) &= -x_0^2 \cos(\omega t) - \frac{2x_0 p_0 \sin(\omega t)}{m\omega} - \frac{i\sigma^2 p_0^2 \sin(\omega t)}{m\omega\hbar} \\ &\quad + 2 \left( x_0 + \frac{i\sigma^2 p_0}{\hbar} \right) x \\ &\quad - \left[ \cos(\omega t) + \frac{im\omega\sigma^2 \sin(\omega t)}{\hbar} \right] x^2, \end{aligned} \quad (12)$$

from which the following position and momentum uncertainties can be computed

$$\begin{aligned} \Delta x(t) &= |L(t)|/\sqrt{2}, \\ \Delta p(t) &= \sqrt{\frac{(\hbar/\sigma)^2 \cos^2(\omega t) + (m\omega\sigma)^2 \sin^2(\omega t)}{2}}. \end{aligned} \quad (13)$$

Thus, unless  $\sigma^2 = \hbar/m\omega$ , both of them oscillate with a period equal to half of the natural period of the classical simple harmonic oscillator [4, 23], and so does their product  $\Delta x \Delta p$ . However, for the particular value  $\sigma_{\text{coh}}^2 = \hbar/m\omega$  one finds a so-called coherent state for which the shape of the wave packet does not change in time. Consequently, its width also remains constant in time. One finds  $\Delta x = \sigma_{\text{coh}}/\sqrt{2}$  and  $\Delta p = \hbar/(\sqrt{2}\sigma_{\text{coh}})$  and therefore the product of the uncertainties is time

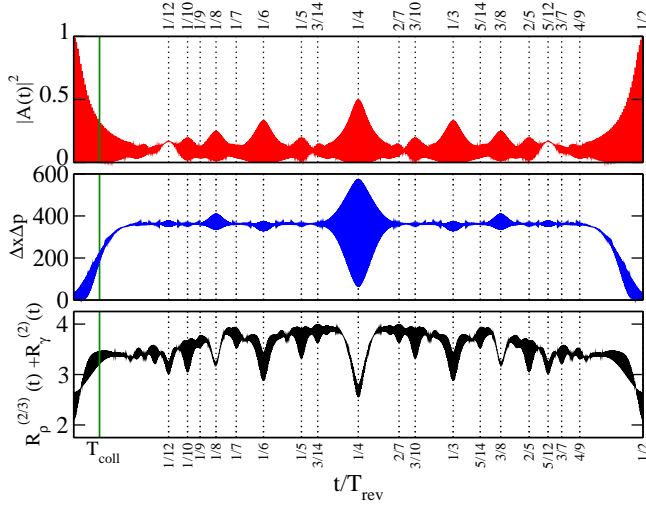


FIG. 1: (color online). Time dependence of (top panel, red curve)  $|A(t)|^2$ , (middle panel, blue curve)  $\Delta x(t)\Delta p(t)$ , and (bottom panel, black curve)  $R_\rho^{(2/3)}(t) + R_\gamma^{(2)}(t)$  for an initial Gaussian wave packet with  $x_0 = L/2$ ,  $p_0 = 400\pi$ , and  $\sigma = \sqrt{2}/10$  in an infinite square-well. The main fractional revivals are indicated by vertical dotted lines, and the vertical, green solid line stands for the collapse time.

independent and equals  $\hbar/2$ , what renders the coherent state a state of minimum uncertainty. This phenomenology is of importance to several fields in quantum mechanics and reflects in the behavior of the Rényi entropies in a clear way. For the harmonic oscillator, the position and momentum Rényi entropies for parameters  $\alpha$  and  $\beta$  can be readily calculated as,

$$R_\rho^{(\alpha)} = \ln(\sqrt{\pi}|L(t)|) - \frac{\ln(\sqrt{\alpha})}{1-\alpha}, \quad (14)$$

$$R_\gamma^{(\beta)} = \ln\left(\frac{\sqrt{\pi}}{|L(t)|}\right) - \frac{\ln(\sqrt{\beta})}{1-\beta}, \quad (15)$$

and hence, when taken separately, they reproduce the classical periodic behavior except for the particular value  $\sigma_{\text{coh}}^2$  for which the Rényi entropies are constants of the motion. In this case, moreover, their sum  $R_\rho^{(\alpha)} + R_\gamma^{(\beta)}$  reaches the lower bound at all times, as expected for a system whose states remain Gaussian-like.

## B. Infinite square well

Consider a particle of mass  $m$  in an infinite potential-well defined as  $V(x) = 0$  for  $0 < x < L$  and  $V(x) = +\infty$  otherwise. The time-dependent wave function for a localized quantum wave packet is expanded as a one-dimensional superposition of energy eigenstates as

$$\psi(x, t) = \sum_n a_n u_n(x) e^{-iE_n t/\hbar}, \quad (16)$$

where the  $u_n(x)$  represent the normalized eigenstates and  $E_n$  the corresponding eigenvalues,

$$u_n(x) \sqrt{\frac{2}{L}} \sin\left(\frac{n\pi x}{L}\right), \quad E_n = \frac{n^2 \hbar^2 \pi^2}{2mL^2}. \quad (17)$$

The infinite square well has exact revivals because the energy levels are integral multiples of a common value (but not equally spaced). The classical and revival periods are  $T_{\text{cl}} = 2mL^2/\hbar\pi n_0$  and  $T_{\text{rev}} = 4mL^2/\hbar\pi$ , respectively [4, 24]. It is easy to see by direct substitution in equation (16) that  $\psi(L-x, t) = -\psi(x, 0)$ , so at a time  $t = T_{\text{rev}}/2$  the initial state reforms exactly, reflected around the center of the well. This is the reason why the time span of the following analysis is  $T_{\text{rev}}/2$  rather than  $T_{\text{rev}}$ .

We shall consider an initial Gaussian wave packet with a width  $\sigma$ , centered at a position  $x_0$  and with a momentum  $p_0$  as in equation (9). Assuming that the integration region can be extended to the whole real axis, the expansion coefficients can be approximated with high accuracy by the analytic expression

$$a_n \approx \sqrt{\frac{4\sigma\pi}{L\sqrt{\pi}}} \frac{e^{-ip_0 x_0/\hbar}}{2i} \left[ e^{in\pi x_0/L} e^{-\sigma^2(p_0 + n\pi\hbar/L)^2/2\hbar^2} - e^{-in\pi x_0/L} e^{-\sigma^2(p_0 - n\pi\hbar/L)^2/2\hbar^2} \right]. \quad (18)$$

To calculate the corresponding time dependent, momentum wave function we use the Fourier transform of the equation (16), that is,

$$\Psi(p, t) = \sum_n a_n \phi_n(p) e^{-iE_n t/\hbar} \quad (19)$$

where

$$\phi_n(p) = \sqrt{\frac{\hbar}{\pi L}} \frac{p_n}{p^2 - p_n^2} \left[ (-1)^n e^{ipL/\hbar} - 1 \right], \quad (20)$$

with  $p_n = \hbar\pi n/L$ . Without loss of generality, we shall henceforth take  $2m = \hbar = L = 1$ ,  $\sigma = \sqrt{2}/20$ , and  $x_0 = L/2 = 0.5$  for the initial wave packet. In our exemplary cases, we use  $p_0 = 400\pi$  to obtain an appropriate relative time scale.

In figure 1 we show the manifestation of fractional revivals with different tools: the usual autocorrelation function (top panel), the expectation-value uncertainty product  $\Delta x \Delta p$  (middle panel), and the sum of Rényi entropies with  $\alpha = \frac{2}{3}$ ,  $\beta = 2$  (bottom panel). At early times, the Gaussian wave packet evolves quasiclassically but in a few periods begins to delocalize and spreads almost uniformly across the entire well. This is the so-called collapse phase. The time-scale for this collapse has been estimated by means of an expectation value analysis to be [4, 25]

$$T_{\text{coll}} = \frac{1}{\sqrt{6}} \frac{mL\sigma}{\hbar} \simeq 0.0144 \quad (21)$$

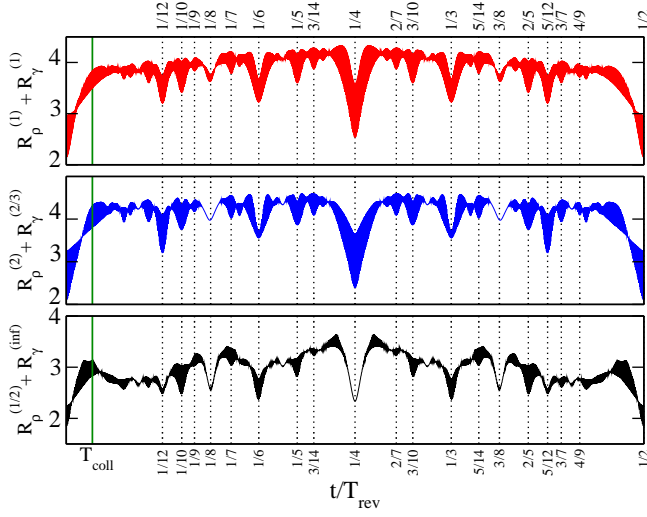


FIG. 2: (color online). Time dependence of (top panel, red curve)  $R_\rho^{(1)}(t) + R_\gamma^{(1)}(t)$  (Shannon entropy), (middle panel, blue curve)  $R_\rho^{(2)}(t) + R_\gamma^{(2/3)}(t)$ , and (bottom panel, black curve)  $R_\rho^{(1/2)}(t) + R_\gamma^{(\text{inf})}(t)$  for an initial Gaussian wave packet in an infinite square-well. The main fractional revivals are indicated by vertical dotted lines and the vertical green curve stands for the collapse time. Parameters as in Fig. 1.

for the set of parameters defined above. It is marked by the solid green line of figure 1, and coincides with the first maximum of the sum of Rényi entropies. By contrast, neither the autocorrelation function nor the curve for the position-momentum uncertainty show any significant feature at  $T_{\text{coll}}$ .

At later times, the system undergoes a sequence of fractional revivals, the most important of which are shown by vertical dotted lines. It can be observed that the sum of Rényi entropies accounts for them in the form of relative minima, only reaching the lower bound at the revival times. As shown in [12], cases can be found within the infinite square well where the autocorrelation function fails to detect fractional revivals whereas the sum of entropies does, the reason being that information entropies take into account the individual subpackets the initial wave packet breaks up into, irrespective of their relative positions. Additionally, it is shown here that the uncertainty relation for position and momentum also captures the main fractional revivals, even though in a much less clear fashion (see, for instance, the fractional revivals occurring at  $t = 1/10$  or  $t = 1/5$ ). The time evolution of the uncertainty product was first used to study the evolution of wave packets in the context of revival phenomena in [5]. The fact that the expectation value analysis gives a poorer description than the entropic one suggests that the formulation of the uncertainty principle in term of Rényi entropies is indeed stronger than that of the standard Heisenberg relation [19, 26].

In contrast to the Shannon entropy, the Rényi entropy has a free parameter and in figure 2 it is shown how the fractional revivals show up in three representative cases:

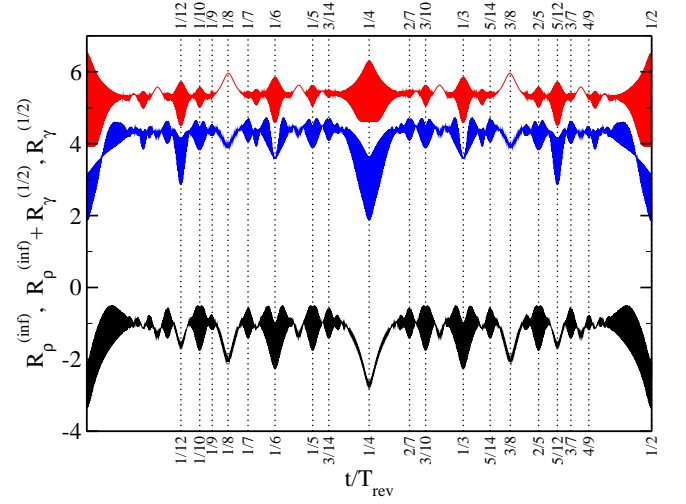


FIG. 3: (color online). Time dependence of (top red curve)  $R_\gamma^{(1/2)}(t)$ , (middle blue curve)  $R_\rho^{(\text{inf})}(t) + R_\gamma^{(1/2)}(t)$ , and (bottom black curve)  $R_\rho^{(\text{inf})}(t)$  for an initial Gaussian wave packet in an infinite square-well. The main fractional revivals are indicated by vertical dotted lines. Parameters as in Fig. 1

the top panel corresponds to  $\alpha = 1, \beta = 1$ , that is, to the sum of Shannon entropies [12]; the middle panel corresponds to the ‘unspecial’ case  $\alpha = 2, \beta = 2/3$ ; the bottom panel corresponds to  $\alpha = 1/2, \beta = \infty$ . Notice that in this latter case  $R_\gamma^{(\text{inf})} = -\ln[\max_p |\phi(p)|^2]$ . Although the three cases reported here yield similar results, it cannot be discarded that the freedom in choosing, say,  $\alpha$  may be used with advantage in some specific cases. The vertical, green solid line indicates again that collapse time-scales can be estimated within the entropic approach as the first maximum of the sum of entropies.

In figure 3 we illustrate the importance of taking the sum of the entropies as an indicator of fractional revivals, and not either of them separately. The top curve corresponds to  $R_\gamma^{(1/2)}$ , the bottom curve to  $R_\rho^{(\text{inf})} = -\ln[\max_x |\psi(x)|^2]$  (which owes its wavy-looking appearance to the presence of the max operator), and the middle one to their sum. It is only the sum of the entropies that embraces both the configurational and dynamical aspects of the wave packet evolution through the uncertainty relation.

### C. Quantum bouncer

Next, consider a particle bouncing on a hard surface under the influence of gravity, that is, a particle in a potential  $V(z) = mgz$ , if  $z > 0$  and  $V(z) = +\infty$  otherwise. The eigenfunctions and eigenvalues are given by [27]

$$\tilde{E}_n = z_n; \quad u_n(\tilde{z}) = \mathcal{N}_n \text{Ai}(\tilde{z} - z_n); \quad n = 1, 2, 3, \dots \quad (22)$$

where  $l_g = (\hbar/2gm^2)^{1/3}$  is a characteristic gravitational length,  $\tilde{z} = z/l_g$ ,  $\tilde{E} = E/mgl_g$ ,  $\text{Ai}(z)$  is the Airy func-

tion,  $-z_n$  denotes its zeros, and  $\mathcal{N}_n = |\text{Ai}'(-z_n)|^{-1}$  [28] is the  $u_n(\tilde{z})$  normalization factor. In the remainder of this paper the tildes on the energy and position variables will be omitted.  $z_n$  and  $N_n$  were determined numerically by using scientific subroutine libraries for the Airy function, although accurate analytic approximations for them can be found in [27]. We have verified that the numeric approach yields slightly better results. The corresponding coefficients of the wave function can be obtained analytically as [28]

$$a_n = \mathcal{N}_n \left( 2^{3/2} \pi \sigma \right)^{1/4} \text{Ai} \left( z_0 - z_n + \frac{\sigma^4}{6} \right) e^{\frac{\sigma^2}{2} \left( z_0 - z_n + \frac{\sigma^4}{6} \right)}. \quad (23)$$

Consider now an initial Gaussian wave packet localized at a height  $z_0$  above the floor, with a width  $\sigma$  and an initial momentum  $p_0 = 0$ . The classical period can be calculated to obtain  $T_{\text{cl}} = 2\sqrt{z_0}$ . As for the revival time, the state  $n_0$  around which the initial wave packet is peaked can be identified via  $z_0 = E_{n_0}$  with the help of  $z_n \simeq [3\pi(4n-1)/8]^{2/3}$  [27]. One finds by direct substitution  $T_{\text{rev}} = 2h/|E''_{n_0}| = 8z_0^2/\pi$ , but it can be shown that at a time half of this value the wave packet reforms half of period out of phase with the classical motion (see [27]). Therefore, we henceforth take  $T_{\text{rev}} = 4z_0^2/\pi$ . The temporal evolution of the wave packet in momentum-space was obtained numerically by the fast Fourier transform method.

We have computed the temporal evolution of the uncertainty product  $\Delta x \Delta p$  and the sums of Rényi entropies  $R_\rho^{(2)} + R_\gamma^{(2/3)}$  and  $R_\rho^{(\text{inf})} + R_\gamma^{(1/2)}$  for the initial conditions  $z_0 = 100$ ,  $\sigma = 1$  and  $p_0 = 0$ . Figure 4 displays these quantities and the location of the main fractional revivals. The top panel shows that  $\Delta x(t) \Delta p(t)$  decreases and reaches a minimum at some fractional revivals. Analogous behavior is seen in the middle and bottom panels for the sum of Rényi entropies. The description in these latter cases is somewhat more complete. Also shown in the same figure is the collapse time-scale  $T_{\text{coll}} = T_{\text{cl}}^3/(4\sqrt{2}\sigma) \simeq 1414.21$  located close to the maximum entropy area [27].

### III. SUMMARY

In this paper we have generalized and expanded on the entropic approach put forward in [12] by using Rényi uncertainty relations to study revival behavior in three

model systems, namely, the simple harmonic oscillator, the infinite square well, and the quantum bouncer. We have found that they provide a useful framework for visualizing fractional revivals, alternative to the usual autocorrelation function and expectation value analyses.

Additionally, we have also successfully used the standard variance-based uncertainty product to search for the fractional revivals, but the information entropy turns out

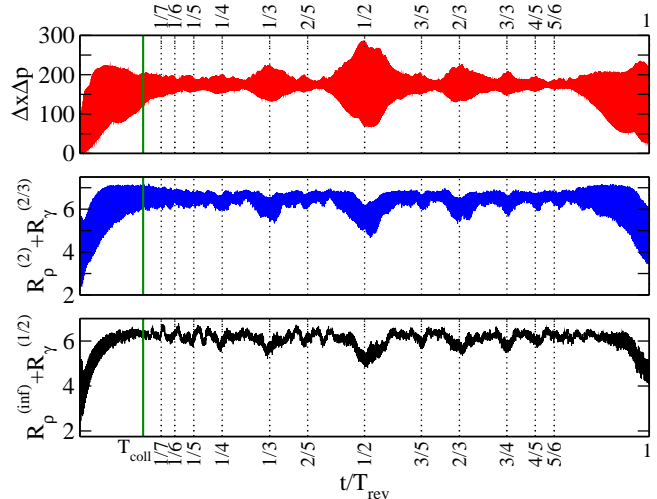


FIG. 4: (color online). Time dependence of (top panel, red curve)  $\Delta x(t) \Delta p(t)$ , (middle panel, blue curve)  $R_\rho^{(2)}(t) + R_\gamma^{(2/3)}(t)$ , and (bottom panel, black curve)  $R_\rho^{(\text{inf})}(t) + R_\gamma^{(1/2)}(t)$  for an initial Gaussian wave packet with  $z_0 = 100$ ,  $p_0 = 0$ , and  $\sigma = 1$  in a quantum bouncer. The main fractional revivals are indicated by vertical dotted lines, and the vertical, green solid line stands for the collapse time.

tribution. We have also shown that collapse time-scales can also be computed within the entropic approach. In summary, we have shown that entropic uncertainty relations are a good tool to investigate properties of the temporal evolution of wave packets.

### IV. ACKNOWLEDGMENTS

This work was supported in part by the Spanish projects FIS2005-00973 (Ministerio de Ciencia y Tecnología), FQM-2725 and FQM-165 (Junta de Andalucía).

- 
- [1] J.H. Eberly, N.B. Narozhny, and J.J. Sánchez-Mondragón, Phys. Rev. Lett. **44**, 1323 (1980).
  - [2] I.Sh. Averbukh and J.F. Perelman, Phys. Lett. A **139**, 449 (1989); Acta Phys. Pol. **A78**, 33 (1990).
  - [3] D.L. Aronstein and C.R. Stroud Jr., Phys. Rev. A **55**, 4526 (1997).

- [4] R.W. Robinett, Phys. Rep. **392**, 1 (2004).
- [5] J.A. Yeazell, M. Mallalieu, and C.R. Stroud, Jr., Phys. Rev. Lett. **64**, 2007 (1990).
- [6] G. Rempe, H. Walther, and N. Klein, Phys. Rev. Lett. **58**, 353 (1987); T. Baumert *et al.*, Chem. Phys. Lett. **191**, 639 (1992); M.J.J. Vrakking, D.M. Villeneuve,

- and A. Stolow, Phys. Rev. A **54**, R37-R40 (1996); A. Rudenko *et al.*, Chem. Phys. **329**, 193 (2006).
- [7] I.Sh. Averbukh *et al.*, Phys. Rev. Lett. **77**, 3518 (1996).
- [8] M. Mehring, K. Müller, I.Sh. Averbukh, W. Merkel, and W.P. Schleich, Phys. Rev. Lett. **98**, 120502 (2007); M. Gilowski, T. Wendrich, T. Müller, Ch. Jentsch, W. Ertmer, E.M. Rasel, and W.P. Schleich, Phys. Rev. Lett. **100**, 030201 (2008); D. Bigourd, B. Chatel, W.P. Schleich, and B. Girard, Phys. Rev. Lett. **100**, 030202 (2008).
- [9] C. Sudheesh, S. Lakshmibala, and V. Balakrishnan, Phys. Lett. A **329**, 14 (2004).
- [10] M.A. Donchesk and R.W. Robinett, Am. J. Phys. **69**, 1084 (2001).
- [11] D.L. Aronstein and C.R. Stroud, Jr., Laser Phys. **15**, 1496 (2005).
- [12] E. Romera and F. de los Santos, Phys. Rev. Lett. **99**, 263601 (2007).
- [13] K. Bongs *et al.*, Phys. Rev. Lett. **83**, 3577 (1999).
- [14] B.M. Garraway and K.A. Suominen, Contemp. Phys. **43**, 97 (2002); Ch. Warmuth *et al.*, J. Chem. Phys. **114**, 9901 (2001).
- [15] O. Gühne and M. Lewenstein, Phys. Rev. A **70**, 022316 (2004); G. Adesso, A. Serafini, and F. Illuminati, Phys. Rev. A **70**, 022318 (2004); F.A. Bovino *et al.*, Phys. Rev. Lett. **95**, 240407 (2005); B.M. Terhal, Theor. Comput. Sci. **287**, 313 (2002).
- [16] P. Lay, S. Nagy, and J. Pipek, Phys. Rev. A **72**, 022302 (2005).
- [17] D.G. Arbó *et al.*, Phys. Rev. A **67**, 063401 (2003); S. Gnutzmann and K. Zyczkowski, J. Phys. A: Math. Gen. **34**, 10123 (2001); F. Verstraete and J.I. Cirac, Phys. Rev. B **73**, 094423 (2006).
- [18] C. Beck and D. Graudenz, Phys. Rev. A **46**, 6265 (1992); S. Kohler and P. Hänggi, in Quantum Information Processing, edited by G. Leuchs and T. Beth (Wiley-VCH, Berlin, 2002).
- [19] I. Białynicki-Birula, Phys. Rev. A **74**, 052101 (2006).
- [20] I. Białynicki-Birula and J. Mycielski, Comm. Math. Phys. **44**, 129 (1975); W. Beckner, Ann. Math. **102**, 159 (1975).
- [21] E.H. Kennard, Z. Phys. **44**, 326 (1927).
- [22] R. Bluhm, V. A. Kosteletzky and J.A. Porter, Am. J. Phys. **64**, 944 (1996).
- [23] D.F. Styer, Am. J. Phys. **58**, 742 (1990).
- [24] D.L. Aronstein and C.R. Stroud, Jr., Phys. Rev. A **55**, 4526 (1997).
- [25] R.W. Robinett, Am. J. Phys. **68**, 410 (2000).
- [26] H. Maasen and J.B.M. Uffink, Phys. Rev. Lett. **60**, 1103 (1988); J.B.M. Uffink, Ph. D. Thesis, University of Utrecht, 1990 (unpublished) (<http://www.phys.uu.nl/igg/jos/publications/proefschrift.pdf>).
- [27] J. Gea-Banacloche, Am. J. Phys. **67**, 776 (1999).
- [28] O. Vallée, Am. J. Phys. **68**, 672 (2000).